https://doi.org/10.4047/jap.2022.14.6.369

Three-dimensional analysis of the outcome of different scanning strategies in virtual interocclusal registration

Jiansong Mei[1,2], Liya Ma[1,2], Jiarui Chao[1,2], Fei Liu[1,2], Jiefei Shen[1,2]*

[1]State Key Laboratory of Oral Diseases, National Clinical Research Center for Oral Diseases, National Center for Stomatology, West China School of Stomatology, Sichuan University, Chengdu, China
[2]Department of Prosthodontics, West China Hospital of Stomatology, Sichuan University, Chengdu, China

ORCID
Jiansong Mei
https://orcid.org/0000-0003-1610-7390
Liya Ma
https://orcid.org/0000-0001-7800-3568
Jiarui Chao
https://orcid.org/0000-0002-9210-1989
Fei Liu
https://orcid.org/0000-0002-7205-5655
Jiefei Shen
https://orcid.org/0000-0003-0070-1475

Corresponding author
Jiefei Shen
Department of Prosthodontics, West China Hospital of Stomatology, Sichuan University, No. 14, Section 3, Renmin South Road, Chengdu 610041, Sichuan, China
Tel +86-28-85501455
E-mail shenjiefei@scu.edu.cn

Received July 29, 2022 /
Last Revision November 1, 2022 /
Accepted December 11, 2022

This study was supported by National Science and Technology Support Program Project of China (2015BAH13F02).

PURPOSE. The purpose of this *in vitro* study was to assess whether scanning strategies of virtual interocclusal record (VIR) affect the accuracy of VIR during intraoral scanning. **MATERIALS AND METHODS.** Five pairs of reference cubes were added to the digital upper and lower dentitions of a volunteer, which were printed into resin casts. Subsequently, the resin casts were articulated in the maximal intercuspal position in a mechanical articulator and scanned with an industrial computed tomography system, of which the VIR was served as a reference VIR. The investigated VIR of the upper and lower jaws of the resin master cast were recorded with an intraoral scanner according to 9 designed scanning strategies. Then, the deviation between the investigated VIRs and reference VIR were analyzed, which were measured by the deviation of the distances of six selected reference points on the upper reference cubes in each digital cast to the XY-plane between the investigated VIRs and reference VIR. **RESULTS.** For the deviation in the right posterior dentitions, RP group (only scanning of right posterior dentitions) showed the smallest deviation. Besides, BP group (scanning of bilateral posterior dentitions) showed the smallest deviation in the left posterior dentitions. Moreover, LP group (scanning of left posterior dentitions) showed the smallest deviation in the anterior dentitions. For the deviation of full dental arches, BP group showed the smallest deviation. **CONCLUSION.** Different scanning strategies of VIR can influence the accuracy of alignment of virtual dental casts. Appropriate scanning strategies of VIR should be selected for different regions of interest and edentulous situations. [J Adv Prosthodont 2022;14:369-78]

KEYWORDS
Intraoral scanner; Virtual interocclusal registration; Virtual interocclusal record; Scan strategy; Accuracy

https://doi.org/10.4047/jap.2022.14.6.369

INTRODUCTION

The rapid development of intraoral scanner (IOS) in dentistry has led to a shift to a digital approach for creating impressions[1,2] and interocclusal registration from the conventional method using polyvinyl siloxane or bite wax.[3-5] Beside the precise virtual dental casts,[6-8] the virtual interocclusal record (VIR) of the maxillary and mandibular dentitions is also important for digital dental treatments.[9,10] The VIR is one or several 3D records that register the relationship between the maxillary and mandibular in the proposed occlusal position, such as the maximal intercuspal position (MIP).[11] With VIRs, digital maxillary and mandibular casts obtained from IOS can be repositioned in the CAD software program for the treatment design,[11-13] for instance, implant surgical template design[7], dental prosthetic fabrication,[14,15] and planning of orthodontic treatment.[16] Therefore, inaccurate VIR can affect the effect of corresponding dental treatments.

The accuracy of VIR can be affected by the span of scanning with IOS. For example, occlusal contacts obtained from VIR based on the quadrant scans are different from those based on the complete-arch scans.[17,18] The accuracy of VIR can also be influenced by the section quantity. For instance, an *in vitro* study performed by Solaberrieta *et al*.[12] has indicated that the combination of the right and the left lateral sections are suggested to obtain a more accurate interocclusal record. However, the study used an industrial 3-dimensional scanner to digitize the casts and obtained the VIRs according to the scan sections formed by cutting the full dentition scan of VIR into a different number of sections. Thus, the results do not necessarily equate with those obtainable by the IOS. Furthermore, whether the scanning direction of VIR can affect the accuracy of VIR is still unclear.

Therefore, this study *in vitro* was performed to further investigate the effect of different scanning strategies with different scanning section quantities, spans, and directions on the accuracy of VIR during intraoral scanning. The null hypothesis that the accuracy of VIR would not be affected by the scanning strategies.

MATERIALS AND METHODS

This study was approved by the West China Hospital of Stomatology Institutional Review Board (IRB: WCHSIRB-D-2020-389). In order to obtain a pair of digital casts of maxillary and mandibular dentition with stable MIP for the sample preparation of this study, the maxillary and mandibular dentition of one volunteer (male aged 20, with full dentition, stable MIP, normal overjet, and overbite) were scanned by the IOS (TRIOS 3; 3Shape, Copenhagen, Denmark). The digital casts were exported as Standard Tessellation Language (STL) files.

The workflow of the following *in vitro* study was described in Figure 1. Briefly, to prepare the above virtual maxillary and mandibular casts for measurement and analysis, five pairs of reference cubes (named cubes 1-10) were added on the labial/buccal gingival surface of the virtual maxillary and mandibular casts in Geomagic 15.0 (3D systems; Wilsonville, OR, USA), respectively (Fig. 1A). To establish a XY-plane for the following measurement and analysis, the upper surface of the five mandibular reference cubes (cubes 1-5) were located on the same plane with lateral surfaces paralleled with each other. Next, the STL files of the upper and lower virtual master casts with reference cubes were printed into master casts of acrylic resin by a 3D printer (DLP1080E; Han's Laser, Shenzhen, China). Subsequently, the above resin upper and lower master casts were articulated in MIP determined by the full dentition in an articulator (Artex CPR; Amann Girrbach, Pforzheim, Germany), (Fig. 1B). Then, the articulator was locked in the hinge movement, preventing mandibular deviation during jaw closure. To establish the reference data, the whole maxillary and mandibular resin casts fixed in the MIP by the articulator were scanned by an industrial computed tomography (CT) system (Metrotom 1500G3; Zeiss, Oberkochen, Germany) with high precision (Fig. 1C), which were then exported as an STL file. The investigated VIRs of the upper and lower jaws of the resin master cast were recorded with an IOS (Fig. 1D) according to 9 designed scanning strategies. For the analysis of the deviation between the investigated VIRs and the reference VIR, the distances of six selected reference points on the upper reference cubes in

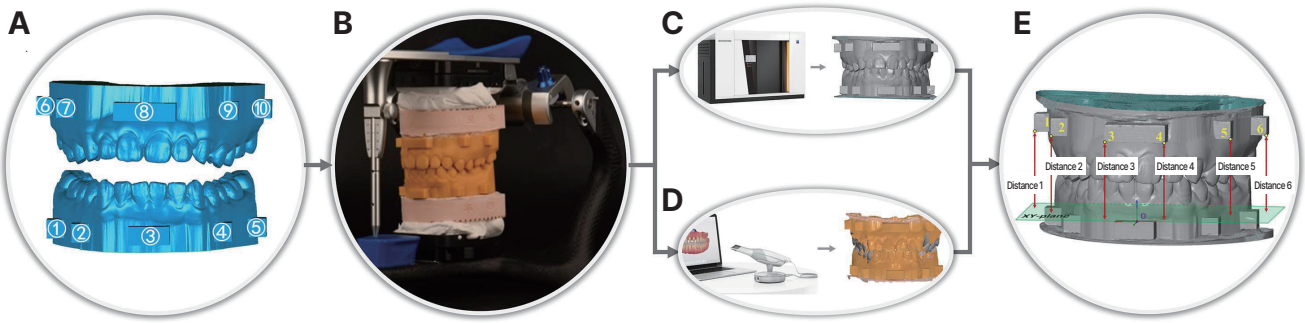

Fig. 1. Workflow of the study. (A) virtual master casts with reference cubes 1 to 10, (B) resin master casts fixed by articulator, (C) reference cast of MIP recording obtained by industrial CT system, (D) study groups obtained by IOS, (E) analysis of deviations in the distance of the six pairs of reference points between the study groups and reference cast.

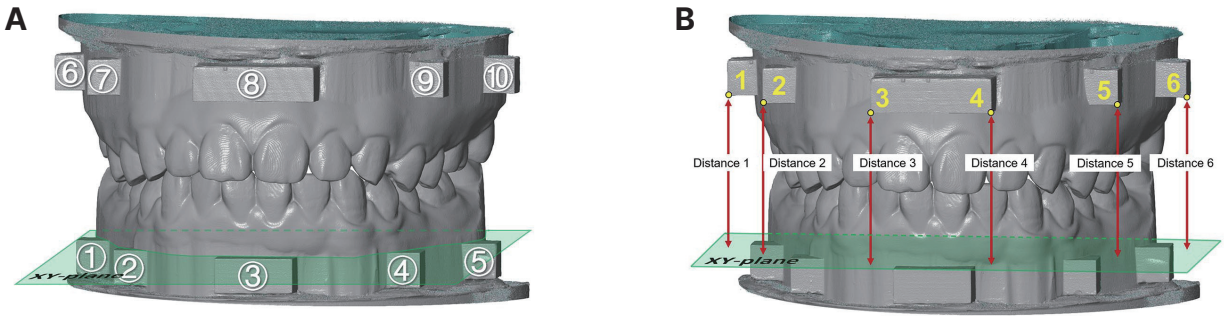

Fig. 2. Construction of the measuring parameters. (A) The XY-plane was constructed by the upper surface of cubes 1-5, (B) distances 1-6 were measured between reference points 1-6 and their corresponding projection points on XY-plane. The white numbers 1-10 indicate the reference cubes 1-10, the green planes indicate the fitting planes, the yellow points in the maxillary cast indicate the 6 reference points, and red line segment indicate the distances 1-6.

each digital cast to the XY-plane were constructed (Fig. 1E).

The XY-plane was constructed by the upper surface of the five mandibular reference cubes (cubes 1-5) (Fig. 2A). Then, 6 reference points (named points 1-6), three-plane intersection points of a reference cube, were selected on the five maxillary reference cubes (cubes 6-10), and their distance (named distances 1-6) to the XY-plane was measured in the Inspect 2020 software (GOM; Zeiss, Oberkochen, Germany) as a control (Fig. 2B).

In study groups, the upper and lower resin casts articulated in the articulator were scanned once using the IOS without rescanning procedure in accordance with the manufacturer's instructions. Next, based on the different scanning strategies of the VIR of the upper and lower resin casts in the MIP articulated in the articulator, 9 study groups were designed and displayed in Figure 3, including the right posterior (RP) group, left posterior (LP) group, bilateral posterior (BP) group, right quadrant (RQ) group, left quadrant (LQ) group, bilateral quadrant (BQ) group, complete arch 1 (CA1) group, complete arch 2 (CA2) group, and anterior (ANT) group. The VIR of each group was taken and repeated 10 times by scanning the upper and lower dentition but not the reference cubes. Finally, the upper and lower jaws in the MIP were exported into STL files by Trios 3 software. Then, the 90 samples of STL files of the 9 study groups were imported into the Inspect 2020 software, respectively. The corresponding distances 1-6 in the 90 samples from the 9 study groups were also measured by the same meth-

https://doi.org/10.4047/jap.2022.14.6.369

od as described above.

Then, the deviations of distances 1-6 between the control and each sample from the 9 study groups were calculated and named δ1 to δ6, respectively. The mean value of δ1 and δ2 represented the deviation of the right posterior dentition of each sample, named δR. The mean value of δ3 and δ4 represented the deviation of the anterior dentition of each sample, named δA. The mean value of δ5 and δ6 represented the deviation of the left posterior dentition of each sample, named δL. In addition, the mean value of δ1-δ6 of each sample was calculated and named δD. Finally, δR, δA, δL, and δD were compared among the 9 study groups, respectively.

Shapiro-Wilk test was applied to test the distribution of δR, δA, δL, and δD, and the results demonstrated that these variables were non-normally distributed. Then the Kruskal-Wallis test was used to detect the difference of δR, δA, δL, and δD among the 9 groups. Besides, the Bonferroni correction was used to prevent increased type I error during the post hoc test for pair-wise comparisons. The significant levels of all analyses were set at .05.

RESULTS

Statistically significant differences in δR, δA, δL, and δD were found among the study groups. Tables 1 to 4 list the median and interquartile range of δR, δA, δL, and δD. When comparing the difference in the devia-

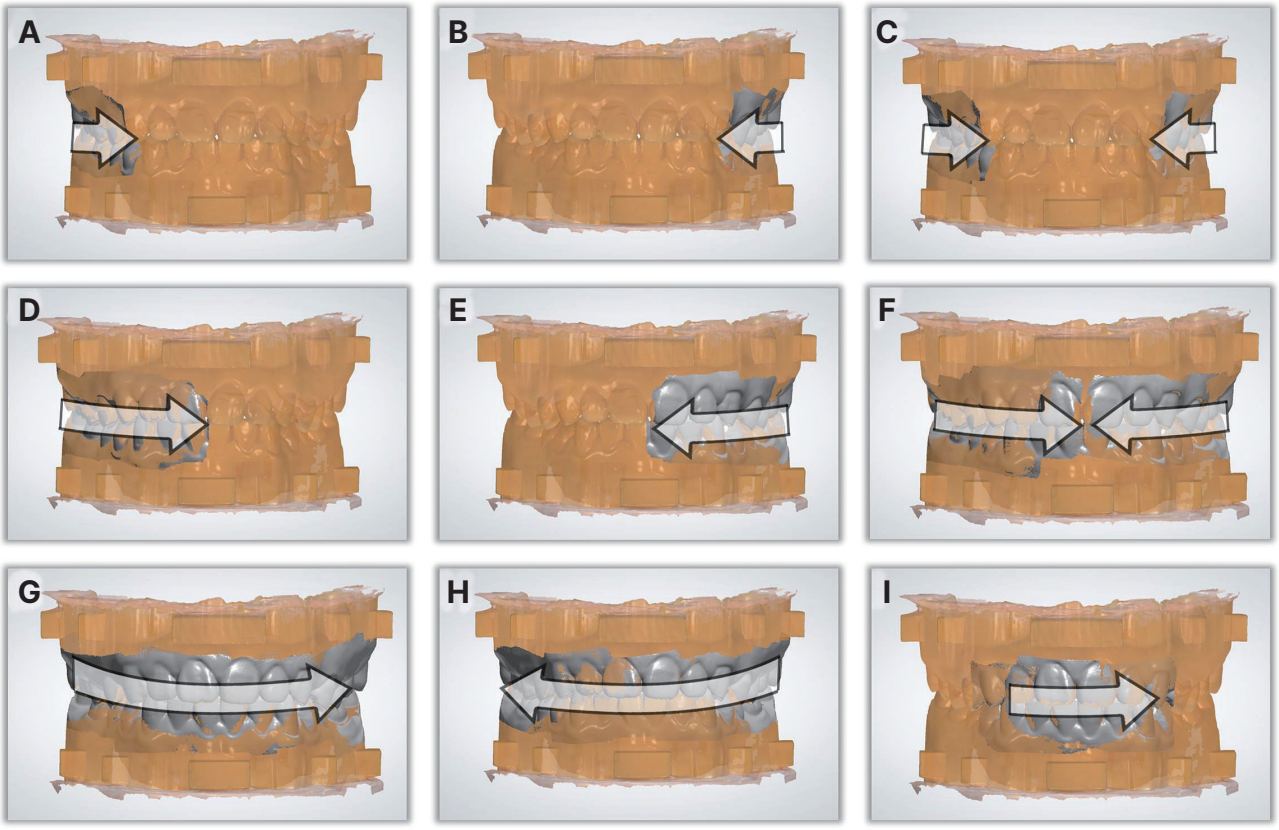

Fig. 3. The scanning strategies of 9 study groups. (A) RP group, 1 section, from right 2nd molar to ipsilateral 1st premolar, (B) LP group, 1 section, from left 2nd molar to ipsilateral 1st premolar, (C) BP group, 2 sections, from 2nd molar to ipsilateral 1st premolar bilaterally (D) RQ group, 1 section, from right 2nd molar to ipsilateral central incisor. (E) LQ group, 1 section, from left 2nd molar to ipsilateral central incisor, (F) BQ group, 2 sections, from 2nd molar to ipsilateral central incisor bilaterally, (G) CA1 group, 1 section, from right 2nd molar to left 2nd molar, (H) CA2 group, 1 section, from left 2nd molar to right 2nd molar, (I) ANT group, 1 section, right canine to left canine. The white arrows indicate the span and scanning direction of VIR.

tion of the right posterior dentition among the 9 study groups, the RP group showed the smallest median δR, which was significantly smaller compared to the other groups ($P < .05$) except the RQ, BP, and BQ groups ($P > .05$) (Table 1 and Fig. 4A). When comparing the difference in the deviation of the left posterior dentition among the 9 study groups, the BP group showed the lowest median δL which was significantly smaller than the other groups ($P < .05$) except the LP, LQ, and BQ groups ($P > .05$) (Table 2 and Fig. 4B). However, for analysis of the deviation in the anterior dentition in each group, the LP group showed the lowest median δA, which was only significantly smaller than that of the CA2 group ($P < .05$) (Table 3 and Fig. 4C). There was no significant difference in the δA of the LP group when compared with the other groups ($P > .05$). Taking the δD into account which represented the deviation of the full arches, the BP group showed the smallest median δD, which was only significantly smaller than that of the CA2 and CA1 groups ($P < .05$) (Table 4 and Fig. 4D).

When comparing the difference in the deviation of the right and left posterior dentition in RP, RQ, LP, and LQ groups, the δR was significantly smaller than δL in the RP and RQ groups ($P < .05$) (Fig. 5A, B). In the LP group, the δL is significantly smaller than δR ($P < .05$) (Fig. 5C). But there was no significant difference between the δL and δR in the LQ group ($P > .05$) (Fig. 5D).

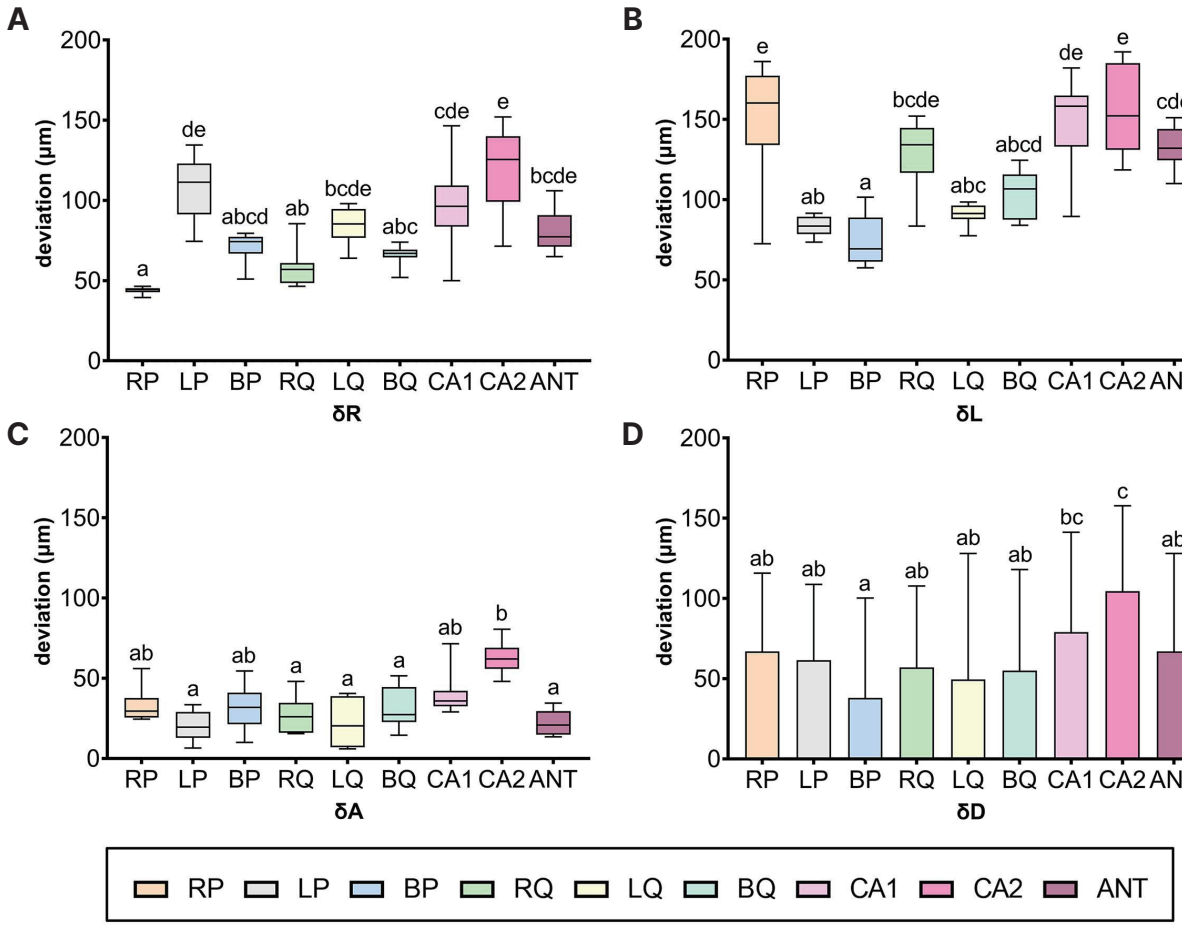

Fig. 4. Box plot demonstrating accuracy measurement reflecting δR, δA, δL, and δD with different scanning strategies of VIR. Median, interquartile range, minimum and maximum values (μm) of δR, δA, δL, and δD, (A) δR represented with box plot, (B) δL represented with box plot, (C) δA represented with box plot, (D) δD represented with box plot. No same superscript letters (a-e) on the box plot indicating there is a significant difference among different scanning strategies ($P < .05$).

https://doi.org/10.4047/jap.2022.14.6.369

Table 1. Median, interquartile range, minimum and maximum values (μm) of δR with different scanning strategies of VIR

VIR	Minimum	Q1	Median	Q3	Maximum	Mean	Standard Deviation
RP	39.5	43.75	44.75^{a}	45	46.5	43.9	2.2
LP	74.5	92.875	111.25^{de}	121.5	134.5	106.9	18.89
BP	51	68.75	74.25^{abcd}	76.875	79.5	71.05	8.83
RQ	46.5	50.125	57^{ab}	58.75	85.5	57.95	11.52
LQ	64	78.125	85.25^{bcde}	94.5	98	84.55	11.24
BQ	52	65.25	67^{abc}	68.5	74	66.25	5.91
CA1	50	85	96.25^{cde}	106.125	146.5	96.8	25.32
CA2	71.5	106.5	125.5^{e}	136.375	152	12.05	25.62
ANT	65	72.75	77.25^{bcde}	88	106	81.35	12.67
P-value			< .001				

VIR, virtual interocclusal record; Q1, first quartile; Q3, third quartile; δR, deviation in the sum of moduli of distances 1 and 2 between investigated VIRs and reference VIR; RP, right posterior group; LP, left posterior group; BP, bilateral posterior group; RQ, right quadrant group; LQ, left quadrant group; BQ, bilateral quadrant group; CA1, complete arch 1 group; CA2, complete arch 2 group; ANT, anterior group. No same superscript letters (a-e) in the "Median" column indicating there is a significant difference among different scanning strategies ($P < .05$).

Table 2. Median, interquartile range, minimum and maximum values (μm) of δL with different scanning strategies of VIR

VIR	Minimum	Q1	Median	Q3	Maximum	Mean	Standard Deviation
RP	72.5	145.25	160.25^{e}	174.625	186	151.65	35.87
LP	73.5	79.25	83.5^{ab}	88.75	91.5	83.8	5.93
BP	57.5	62.25	69.25^{a}	83.125	101.5	73.65	15.62
RQ	83.5	123.625	134.25^{bcde}	141.125	152	128.9	21.52
LQ	77.5	88.75	91.25^{abc}	95.625	98.5	91	6.2
BQ	84	88.75	106.75^{abcd}	113.125	124.5	103.25	14.46
CA1	89.5	134.375	158.25^{de}	160.25	182	148.55	27.19
CA2	118.5	135.125	152.25^{e}	176.875	192	154	27.43
ANT	110	127	132^{cde}	139.625	151	132.85	12.62
P-value			< .001				

VIR, virtual interocclusal record; Q1, first quartile; Q3, third quartile; δL, deviation in the sum of moduli of distances 5 and 6 between investigated VIRs and reference VIR; RP, right posterior group; LP, left posterior group; BP, bilateral posterior group; RQ, right quadrant group; LQ, left quadrant group; BQ, bilateral quadrant group; CA1, complete arch 1 group; CA2, complete arch 2 group; ANT, anterior group. No same superscript letters (a-e) in the "Median" column indicating there is a significant difference among different scanning strategies ($P < .05$).

Table 3. Median, interquartile range, minimum and maximum values (μm) of δA with different scanning strategies of VIR

VIR	Minimum	Q1	Median	Q3	Maximum	Mean	Standard Deviation
RP	24.5	25.75	29.5^{ab}	36.25	56	32.5	9.64
LP	6.5	13.125	19.5^{a}	26.875	33.5	20.1	9.22
BP	10	25.125	31.75^{ab}	39.25	54.5	31.25	14.28
RQ	15.5	16.125	26^{a}	33.875	48	26.55	11.21
LQ	6	7.375	20.25^{a}	34	40.5	20.85	14.23
BQ	14.5	24.125	27.25^{a}	41.875	51.5	31.3	12.39
CA1	29	33.5	35.75^{ab}	40.25	71.5	39.05	12.32
CA2	48	57.125	62^{b}	67.375	80.5	62.7	9.41
ANT	13.5	15.5	20.75^{a}	27.75	34.5	21.7	7.36
P-value			< .001				

VIR, virtual interocclusal record; Q1, first quartile; Q3, third quartile; δA, deviation in the sum of moduli of distances 3 and 4 between investigated VIRs and reference VIR; RP, right posterior group; LP, left posterior group; BP, bilateral posterior group; RQ, right quadrant group; LQ, left quadrant group; BQ, bilateral quadrant group; CA1, complete arch 1 group; CA2, complete arch 2 group; ANT, anterior group. No same superscript letters (a-b) in the "Median" column indicating there is a significant difference among different scanning strategies ($P < .05$).

Table 4. Median, interquartile range, minimum and maximum values (μm) of δD with different scanning strategies of VIR

VIR	Minimum	Q1	Median	Q3	Maximum	Mean	Standard Deviation
RP	4	15.5	67^{ab}	113.25	223	76.02	65.63
LP	2	31.75	61.5^{ab}	108.25	182	70.27	47.92
BP	0	29.75	38^{a}	96.75	129	58.65	40.34
RQ	2	17.75	57^{ab}	107.25	195	71.13	57.29
LQ	1	27.5	49.5^{ab}	124	146	65.47	49.17
BQ	1	23.5	55^{ab}	118	170	66.93	49.14
CA1	7	46.75	79^{bc}	139.75	218	94.8	59.6
CA2	25	67.75	104.5^{c}	157.25	228	112.25	52.39
ANT	1	27	67^{ab}	128	190	78.63	58.38
P-value			< .001				

VIR, virtual interocclusal record; Q1, first quartile; Q3, third quartile; δD, deviation in the sum of moduli of distances 1-6 between investigated VIRs and reference VIR; RP, right posterior group; LP, left posterior group; BP, bilateral posterior group; RQ, right quadrant group; LQ, left quadrant group; BQ, bilateral quadrant group; CA1, complete arch 1 group; CA2, complete arch 2 group; ANT, anterior group. No same superscript letters (a-c) in the "Median" column indicating there is a significant difference among different scanning strategies ($P < .05$).

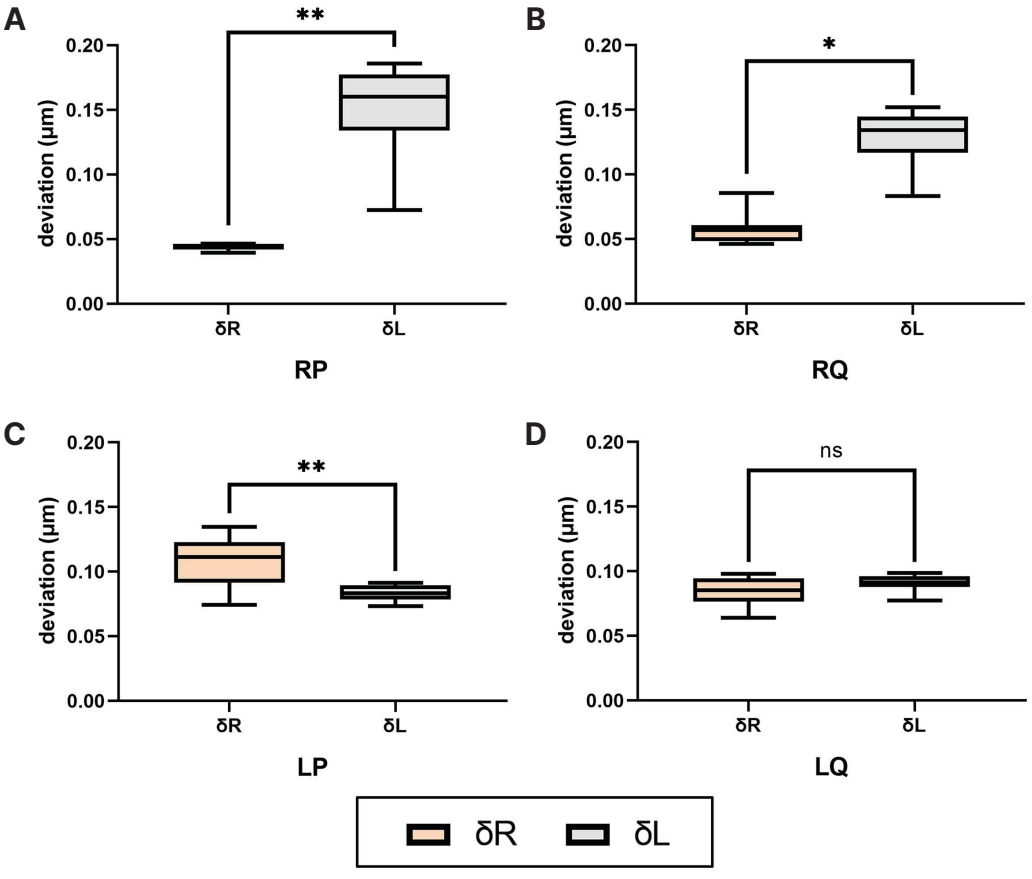

Fig. 5. Box plot demonstrating accuracy measurement between δR and δL in RP, RQ, LP, and LQ groups. Different alphabetical letters indicate statistical differences in different scanning strategies of VIR ($P < .05$). Median, interquartile range, minimum and maximum values (μm) of δR and δL. (A) RP group, (B) RQ group, (C) LP group, (D) LQ group. *: $P < .05$, **: $P < .01$, ns: $P \geq .05$.

https://doi.org/10.4047/jap.2022.14.6.369

DISCUSSION

This study investigated the deviations caused by different scanning strategies with different scanning section quantities, spans, and directions of VIR. The null hypothesis that the accuracy of VIR would not be affected by the scanning strategy was rejected. The VIR error was represented by mean differences between each study group and reference which was obtained by an industrial CT system and proved comparative accuracy in measurement to coordinate measuring machine.[19] These mean differences were compared among study groups at the corresponding distances. The trueness and precision of digital scans for a complete dentate arch have been reported to range between 60 μm and 200 μm.[20,21] The deviations found in the present study are within this reported range.

Several pairs of markers, such as silicone nitride spheres,[15] cobalt chrome molybdenum hemispheres[22] and markers pierced by tungsten carbide,[11] were used in the upper and lower jaws of the dentition as reference points for measurements. In the present study, the fitting planes and three-plane intersection points were constructed on the reference cubes 1-10 by Gaussian best-fit method, preventing the arbitrariness of manual point selection for subsequent measurement and solving the uneven surface of reference cubes after scanning.

In the present study, to minimize the variables that could influence the outcome of virtual interocclusal registration, the virtual relationship between the digital upper and lower casts was established automatically by the IOS software, without any operator intervention. In addition, according to the previous studies,[23-25] the artificial landmarks had a significant effect on the accuracy of the intraoral scanner. In order to eliminate the influence of reference cubes during virtual interocclusal registration, the VIR was taken without including the reference cubes.

For the strategies of obtaining one section of VIR, the results of the present study indicated that the wider span of VIR caused higher deviations. On the contrary, Revilla-León *et al*.[26] have compared the virtual bilateral interocclusal record including 4 teeth with that contained only 2 or 3 teeth and recommended the latter. However, the influence of VIR involving more than 4 teeth was not assessed. In the present study, RP and RQ groups, in which the scanning strategies did not pass the midline, showed significantly smaller δR than the CA1 group with full arch scanning. Similarly, the LP and LQ groups, of which the scanning span was within the left side, showed significantly smaller δL than the CA2 group of full arch scanning, indicating the VIR covering the full dental arch causes higher deviations in the alignment of virtual casts. As IOS systems capture single images of the tooth and produce an assembled virtual model of the whole images, the accuracy of VIR might be affected by the process of stitching the scanned images,[27] which might result in VIR covering the full dental arch causing higher deviations in the alignment of virtual casts.

Notably, Ren *et al*.[11] and Iwaki *et al*.[28] have reported that a single missing tooth in complete arch scanning could not influence the accuracy of VIR. Taking these findings into account, it is better to scan one lateral side of the dental arch for the VIR of the full dentition or dentition with one tooth missing. In addition, CA1 and CA2 showed no significant difference in comparison of the δD, δR, δA, and δL, which indicated that the accuracy of VIR was not influenced by the scanning direction. Moreover, in the RP and RQ groups with VIR covering the right posterior area, the δR is significantly smaller than δL. Similarly, in the LP group, the δL is significantly smaller than δR. Although the δL is not statistically different from δR in the LQ group, Edher *et al*.[17] investigated the occlusal contact points between a complete arch and quadrant arch and reported that there exists a tilting effect toward the site of the VIR of a single section in the full dentition. Therefore, when the site of interest is the unilateral posterior area, it is better to perform the VIR covering the ipsilateral side without crossing the middle line in full dentition or dentition with one missing tooth. For instance, in the prosthodontic treatments of a single crown or implant restoration in the posterior dental arch, the VIR covering the ipsilateral prosthetic area without crossing the midline of the dentition is recommended. Furthermore, there was no significant difference in the δR between the RP and RQ groups or in the δL between the LP and LQ groups. Thus, the VIR scanning of the ipsilateral posterior is recommended

for time-saving. Ren *et al*.[11] found that unilateral and bilateral extended edentulous spans with 3 or more missing posterior teeth and the extended edentulous span in the anterior region all affected the accuracy of VIR. In addition, the significant difference between the δR and δL found in the RP, RQ, and LP groups also indicated that the virtual interocclusal registration is not recommended when multiple teeth are missing in the dental arch, for example, all the right or left anterior and posterior teeth are missing. Due to the higher δR than the RP group and higher δL than the BP group in the ANT group, the virtual interocclusal registration is also not recommended in cases of bilateral posterior teeth missing.

Moreover, different clinical scenarios, such as multiple teeth prepared and partial edentulism, might produce different outcomes when compared with the results of the present study. Further studies are recommended to assess the accuracy of the maxillomandibular relationship when the alignment of the upper and lower digital casts is completed using manual and automatic methods.

Limitations of this study included the *in vitro* design that may not have replicated clinical conditions and that only one IOS system was used. In addition, this study did not explicitly exclude errors from the scanning process of the IOS. Future clinical investigations are required to expand and validate the indications of complete digital workflow with VIR.

CONCLUSION

Based on the findings of this study, the scanning strategies of VIR can affect the alignment of virtual dental casts. In single crown or implant restoration, when focusing on the right posterior of the dental arch, the scanning strategies of BP, BQ, RP, and RQ are recommended. For the left posterior dental arch, the scanning strategies of BP, BQ, LP, and LQ are recommended. When focusing on the anterior region, CA1 and CA2 are not recommended. When the right or left anterior and posterior teeth or bilateral posterior teeth are missing, virtual interocclusal registration is not recommended.

REFERENCES

1. Güth JF, Runkel C, Beuer F, Stimmelmayr M, Edelhoff D, Keul C. Accuracy of five intraoral scanners compared to indirect digitalization. Clin Oral Investig 2017;21:1445-55.
2. Wismeijer D, Mans R, van Genuchten M, Reijers HA. Patients' preferences when comparing analogue implant impressions using a polyether impression material versus digital impressions (Intraoral Scan) of dental implants. Clin Oral Implants Res 2014;25:1113-8.
3. Belur D, Nagy WW. An alternative digital workflow for fabricating a mandibular implant-supported complete fixed dental prosthesis with limited restorative space: A clinical report. J Prosthet Dent 2018;120:1-4.
4. van der Zande MM, Gorter RC, Wismeijer D. Dental practitioners and a digital future: an initial exploration of barriers and incentives to adopting digital technologies. Br Dent J 2013;215:E21.
5. Ries JM, Grünler C, Wichmann M, Matta RE. Three-dimensional analysis of the accuracy of conventional and completely digital interocclusal registration methods. J Prosthet Dent 2022;128:994-1000.
6. Renne W, Ludlow M, Fryml J, Schurch Z, Mennito A, Kessler R, Lauer A. Evaluation of the accuracy of 7 digital scanners: An in vitro analysis based on 3-dimensional comparisons. J Prosthet Dent 2017;118:36-42.
7. Wang ZY, Chao JR, Zheng JW, You M, Liu Y, Shen JF. The influence of crown coverage on the accuracy of static guided implant surgery in partially edentulous models: An in vitro study. J Dent 2021;115:103882.
8. Gómez-Polo M, Piedra-Cascón W, Methani MM, Quesada-Olmo N, Farjas-Abadia M, Revilla-León M. Influence of rescanning mesh holes and stitching procedures on the complete-arch scanning accuracy of an intraoral scanner: An in vitro study. J Dent 2021;110:103690.
9. Freilich MA, Altieri JV, Wahle JJ. Principles for selecting interocclusal records for articulation of dentate and partially dentate casts. J Prosthet Dent 1992;68:361-7.
10. Davies S, Al-Ani Z, Jeremiah H, Winston D, Smith P. Reliability of recording static and dynamic occlusal contact marks using transparent acetate sheet. J Prosthet Dent 2005;94:458-61.
11. Ren S, Morton D, Lin WS. Accuracy of virtual interocclusal records for partially edentulous patients. J

Prosthet Dent 2020;123:860-5.
12. Solaberrieta E, Arias A, Brizuela A, Garikano X, Pradies G. Determining the requirements, section quantity, and dimension of the virtual occlusal record. J Prosthet Dent 2016;115:52-6.
13. Solaberrieta E, Garmendia A, Brizuela A, Otegi JR, Pradies G, Szentpétery A. Intraoral digital impressions for virtual occlusal records: section quantity and dimensions. Biomed Res Int 2016;2016:7173824.
14. Park JH, Kim JE, Shim JS. Digital workflow for a dental prosthesis that considers lateral mandibular relation. J Prosthet Dent 2017;117:340-4.
15. Wong KY, Esguerra RJ, Chia VAP, Tan YH, Tan KBC. Three-dimensional accuracy of digital static interocclusal registration by three intraoral scanner systems. J Prosthodont 2018;27:120-8.
16. Yun D, Choi DS, Jang I, Cha BK. Clinical application of an intraoral scanner for serial evaluation of orthodontic tooth movement: A preliminary study. Korean J Orthod 2018;48:262-7.
17. Edher F, Hannam AG, Tobias DL, Wyatt CCL. The accuracy of virtual interocclusal registration during intraoral scanning. J Prosthet Dent 2018;120:904-12.
18. Arslan Y, Bankoğlu Güngör M, Karakoca Nemli S, Kökdoğan Boyacı B, Aydın C. Comparison of maximum intercuspal contacts of articulated casts and virtual casts requiring posterior fixed partial dentures. J Prosthodont 2017;26:594-8.
19. Villarraga-Gómez H, Lee C, Smith ST. Dimensional metrology with X-ray CT: A comparison with CMM measurements on internal features and compliant structures. Precis Eng 2018;51:291-307.
20. Renne W, Ludlow M, Fryml J, Schurch Z, Mennito A, Kessler R, Lauer A. Evaluation of the accuracy of 7 digital scanners: An in vitro analysis based on 3-dimensional comparisons. J Prosthet Dent 2017;118:36-42.
21. Hayama H, Fueki K, Wadachi J, Wakabayashi N. Trueness and precision of digital impressions obtained using an intraoral scanner with different head size in the partially edentulous mandible. J Prosthodont Res 2018;62:347-52.
22. Schmidt A, Benedickt CR, Schlenz MA, Rehmann P, Wöstmann B. Torsion and linear accuracy in intraoral scans obtained with different scanning principles. J Prosthodont Res 2020;64:167-74.
23. Kanjanasavitree P, Thammajaruk P, Guazzato M. Comparison of different artificial landmarks and scanning patterns on the complete-arch implant intraoral digital scans. J Dent 2022;125:104266.
24. Kim JE, Amelya A, Shin Y, Shim JS. Accuracy of intraoral digital impressions using an artificial landmark. J Prosthet Dent 2017;117:755-61.
25. Abduo J, Elseyoufi M. Accuracy of intraoral scanners: A systematic review of influencing factors. Eur J Prosthodont Restor Dent 2018;26:101-21.
26. Revilla-León M, Alonso Pérez-Barquero J, Zubizarreta-Macho Á, Barmak AB, Att W, Kois JC. Influence of the number of teeth and location of the virtual occlusal record on the accuracy of the maxillo-mandibular relationship obtained by using an intraoral scanner. J Prosthodont 2022 Apr 21. Doi: 10.1111/jopr.13526. Epub ahead of print.
27. Moon YG, Lee KM. Comparison of the accuracy of intraoral scans between complete-arch scan and quadrant scan. Prog Orthod 2020;21:36.
28. Iwaki Y, Wakabayashi N, Igarashi Y. Dimensional accuracy of optical bite registration in single and multiple unit restorations. Oper Dent 2013;38:309-15.